A PSEUDOSPECTRAL METHOD FOR SOLVING THE BLOCH EQUATIONS OF THE POLARIZATION DENSITY IN e^- STORAGE RINGS

Klaus A. Heinemann*, Oleksii Beznosov, James A. Ellison, UNM, Albuquerque, New Mexico
Desmond P. Barber, DESY, Hamburg and UNM
Daniel Appelö, University of Colorado, Boulder, Colorado

INTRODUCTION

We consider the numerical evolution of the Bloch equations of Derbenev and Kondratenko (DK) for the polarization density in high-energy electron storage rings, such as the proposed FCC-ee and CEPC. Equilibrium spin polarization is well characterized by the DK formulas for current rings (see [1] and [2]), but deviations may be important at the high energies we have in mind. We believe these Bloch equations, in three degrees of freedom (DOF), derived in [3] give a more complete description at all energies. The equations are a system of three coupled linear partial differential equations for the three components of the polarization density and include the spin flip polarization effect. Following [4] we formulate the equations in action-angle variables and approximate the Fokker-Planck terms. Our goal is to integrate these equations numerically in order to approximate the equilibrium and compare with the DK formulas.

For 3 DOF the polarization density has $6 + 1$ independent variables. For simplicity, suppose that each of the space-like variables has been discretized on a grid with N grid-points, then the computational cost of each time step will scale no better than $O(N^6)$. The presence of parabolic terms in the governing equations necessitates implicit time stepping and thus solutions of linear systems of equations. For a fully coupled problem this will bring the per time step cost to $O(N^{6q})$, with $1 \leq q \leq 3$, depending on the algorithms used for the linear solve. However, only algorithms with $q \approx 1$ are feasible (for Gaussian elimination $q = 3$). Fortunately, as we outline below, the structure of the equations allow us to group the space-like variables into two groups resulting in a cost that, to leading order, scales as $O(MN^{3q})$.

In the next section we present the full and the reduced Bloch equations and the underlying physics. Then we discuss the details of the numerical algorithm outlined above and the issue of complexity in higher dimensions. Finally we present two numerical results showing a depolarization calculation in 1DOF and spectral convergence in a 2DOF example.

BLOCH EQUATION

In a semiclassical probabilistic description of an electron bunch the spin-orbit dynamics is described by the density matrix function (or spin-1/2 Wigner function) ρ written as

$$\rho(t; z) = f(t; z)\frac{1}{2}\left(I_{2\times 2} + \vec{\sigma} \cdot \vec{P}_{loc}(t; z)\right), \quad (1)$$

where f is the classical phase-space density normalized by $\int f(t; z)dz = 1$ and $\vec{P}_{loc}$ is the local polarization vector.

---

* Corresponding author: heineman@math.unm.edu

The polarization density $\vec{\eta} \equiv f\vec{P}_{loc}$. Here $z = (r, p)$ where r and p are the position and momentum vectors of the phase space and t is the time. Also, $\vec{\sigma}$ is the vector of the three Pauli matrices. Thus $f = Tr[\rho]$ and $\vec{\eta} = Tr[\rho\vec{\sigma}]$. The polarization vector $\vec{P}(t)$ of the bunch is $\vec{P}(t) = \int \vec{\eta}(t, z)dz$. When the particle motion is governed just by a Hamiltonian, as in the case of protons, the phase-space density is conserved along a trajectory so that the polarization density obeys the T-BMT equation along the trajectory. However, if the particles are subject to noise and damping due to synchrotron radiation, the evolution of the density of particles in phase space is more complicated. In fact, neglecting collective effects and after several other approximations, ρ evolves via

$$\partial_t f = L_{FP}(t, z)f, \quad (2)$$
$$\partial_t \vec{\eta} = L_{FP}(t, z)\vec{\eta} + \vec{\Omega}(t, z) \times \vec{\eta} + A(t, z)\vec{\eta}$$
$$+ \vec{g}(t, z)f + \vec{L}(t, z)f, \quad (3)$$

where $\times$ denotes the vector product. The explicit forms of $L_{FP}, \vec{\Omega}, A, \vec{g}$ and $\vec{L}$ are given in [3]. The linear second-order partial differential operator L_{FP} is commonly used for electron synchrotrons and storage rings [5, Section 2.5.4], [6]. This Fokker-Planck operator takes into account the effects of the external fields of the accelerator and of the synchrotron radiation on the orbital motion of the particle. The cross product term with $\vec{\Omega}$ takes into account the Thomas-BMT spin precession effect. The terms $A\vec{\eta}$, $\vec{g}f$ and $\vec{L}(\theta, z)f$ take into account spin flips due to the Sokolov-Ternov formula. In particular A covers the Sokolov-Ternov effect and its Baier-Katkov correction. In fact (3) shows how to include orbital motion and thus is a generalization of the BKS equation [7] from a single orbit to the full phase space. As usual, since it is minuscule compared to all other forces, the Stern-Gerlach effect from the spin onto the orbit is neglected in (2). We call the three equations in (3) the *full Bloch equations*. This terminology reflects the analogy with equations for magnetization in condensed matter [8]. To make the presentation of our discretization of (3) succinct we consider a reduced model with the spin flip terms neglected

$$\partial_t \vec{\eta} = L_{FP}(t, z)\vec{\eta} + \vec{\Omega}(t, z) \times \vec{\eta}. \quad (4)$$

We call (4) the *reduced Bloch equations* and they will be the focus here. For a classical derivation see [9]. The reduced Bloch equations take care of the depolarization effects due to the orbital motion.

The equations (2), (3), (4) can be derived from QED, followed by making the semiclassical approximation of the Foldy-Wouthuysen transformation of the Dirac Hamiltonian and finally making a Markov approximation.

For a numerical discretization of (2)-(4) it is more efficient to pose the equations in polar coordinates, (r_k, ϕ_k) (transformed by first going to action angle variables, [4]) and to parametrize time by the angular azimuth θ. The reduced Bloch equations (4) then become

$$\partial_\theta \vec{\eta} = L_{FP} \vec{\eta} + \mathcal{A}(r_1, ..., r_d, \phi_1, ..., \phi_d, \theta) \vec{\eta}. \quad (5)$$

Here the coupling matrix $\mathcal{A}$ is skew-symmetric and defined by $\mathcal{A}_{12} = -\Omega_3$, $\mathcal{A}_{13} = \Omega_2$, $\mathcal{A}_{23} = -\Omega_1$, and

$$L_{FP} = \frac{L}{2\pi} \sum_{l=1}^{d} \left\{ -b_l \frac{\partial}{\partial \phi_l} + \frac{a_l}{r_l} \frac{\partial}{\partial r_l} r_l^2 + \frac{a_l}{2} \Delta_{r_l, \phi_l} \right\}, \quad (6)$$

$$\vec{\Omega} = \vec{\Omega}^0(\theta) + \sum_{l=1}^{d} r_l [\vec{\Omega}_l^C(\theta) \cos \phi_l + \vec{\Omega}_l^S(\theta) \sin \phi_l]. \quad (7)$$

Here $d \in \{1, 2, 3\}$ is the number of degrees of freedom to be considered, $\Delta_{r, \phi}$ is the Laplacian in polar coordinates and L is the length of the design orbit. For a complete derivation of (6)-(7) with underlying assumptions see [4].

The polarization vector $\vec{P}(\theta)$ of the bunch at time θ is

$$\vec{P}(\theta) = \int f(\theta, z) \vec{P}_{loc}(\theta, z) dz = \int \vec{\eta}(\theta, z) dz, \quad (8)$$

where $z = (r_1, ..., r_d, \phi_1, ..., \phi_d)$ and the polarization is $|\vec{P}(\theta)|$. This is to be compared with the DK formulas [2] elsewhere.

NUMERICAL ALGORITHM

Consider (5) with $d = 1$,

$$\partial_\theta \vec{\eta} = \frac{L}{2\pi} \left\{ -b \frac{\partial}{\partial \varphi} + \frac{a}{r} \frac{\partial}{\partial r} r^2 + \frac{a}{2} \Delta_{r, \varphi} \right\} \vec{\eta} + \mathcal{A}(r, \varphi, \theta) \vec{\eta}, \quad (9)$$

posed on a disk $r \leq r_{max}$, $\varphi \in [0, 2\pi]$. The boundary conditions are periodic in φ and we take r_{max} large enough to impose homogenous Dirichlet boundary conditions at $r = r_{max}$, since the initial condition has compact support.

We seek approximations to $\vec{\eta}$ on a Chebyshev grid in r and a uniform grid in φ,

$$r_i = -\cos\left(\frac{\pi i}{n_r}\right), \quad i = 0, ..., n_r,$$
$$\varphi_j = j \frac{2\pi}{n_\varphi}, \quad j = 1, ..., n_\varphi.$$

and expand it in a Fourier series in the φ direction: $\vec{\eta}(r_i, \varphi_j, \theta) \approx \sum_{k=1}^{n_\varphi} \hat{\eta}_k(r_i, \theta) e^{-\iota k \varphi_j}$.

For the kth Fourier mode we determine $\hat{\eta}_k(r, \theta)$ from

$$\frac{\partial \hat{\eta}_k}{\partial \theta} = \frac{L}{2\pi} a \left(2\hat{\eta}_k + \frac{1}{2}(2r + \frac{1}{r}) \frac{\partial \hat{\eta}_k}{\partial r} + \frac{1}{2} \frac{\partial^2 \hat{\eta}_k}{\partial r^2} \right.$$
$$\left. -\iota k b \hat{\eta}_k - \frac{ak^2}{2r^2} \hat{\eta}_k \right) + [\text{FFT}[\mathcal{A}(r, \varphi, \theta) \vec{\eta}]]_k. \quad (10)$$

Here $[\text{FFT}[fg]]_k$ represents the discrete Fourier transform of the kth Fourier mode of the convolution $\hat{f} * \hat{g}$.

Now denote by $\hat{u}_k(\theta)$ the grid function on the r grid for a fixed mode, i.e. $\hat{u}_k(\theta) = [\hat{u}_k(r_0, \theta), ..., \hat{u}_k(r_{n_r}, \theta)]^T$, describing one of the three components of $\hat{\eta}_k$. Then for each component in (10) we have

$$\frac{d\hat{u}_k}{d\theta} = \{C_1 + C_2(k)\} \hat{u}_k + F_k^u(\vec{\eta}). \quad (11)$$

Here C_1 and $C_2(k)$ are matrices representing the mode independent and mode dependent components of the Fokker-Planck operator

$$C_1 = \frac{L}{2\pi} a \left(2I + (R + \frac{1}{2}R^{-1})D_1 + \frac{1}{2}D_2 \right),$$
$$C_2(k) = \frac{L}{2\pi} \left(-\iota k b I - ak^2(R^{-1})^2 \right),$$

and F_k^u represents the kth mode of the Ω coupling term as well as contributions from boundary conditions in r. Further, I is the identity matrix, $R = \text{diag}(r_0, ..., r_{n_r})$, and D_1 and D_2 are spectral differentiation matrices. The entries of the differentiation matrices are found by the techniques for constructing finite difference approximations of any order of accuracy, for any order of the derivative and on general grids described by Fornberg in [10]. To be precise, the coefficients are computed using a numerically stable recursion relation derived from the Lagrange interpolant associated with the grid points (see also the subroutine weights.f provided in [10]).

To evolve in time we use a second order splitting scheme, see e.g. [11]. Let $\hat{u}_k^\nu = \hat{u}_k(\nu \Delta \theta)$ then, for each mode, we compute

$$\hat{u}_k^* = 2\hat{u}_k^\nu - \frac{1}{2} \hat{u}_k^{\nu-1} + \Delta\theta \left[2(F_k^u(\vec{\eta}^\nu) - F_k^u(\vec{\eta}^{\nu-1})) \right], \quad (12)$$

and solve

$$\left[\frac{3}{2} I - \Delta\theta \{C_1 + C_2(k)\} \right] \hat{u}_k^{\nu+1} = \hat{u}_k^*. \quad (13)$$

Thus at each step we compute $\vec{\eta}^{\nu+1}$ given $\vec{\eta}^\nu$ and $\vec{\eta}^{\nu-1}$. For $d = 2$ and $d = 3$ the algorithm stays the same.

The dominating cost in the step (12) is the computation $\text{FFT}[\mathcal{A}(r, \varphi, \theta) \vec{\eta}]$, for each gridline in r using the fast Fourier transform. The cost of this is $O(n_r n_\varphi \log n_\varphi)$. As indicated in the introduction, the cost of the solve in the step (13) depends on the choice of algorithm but can always be split into an initial cost (e.g. LU-factorization) and a solve cost (e.g. back and forward substitution). Ignoring the startup cost, which can be amortized over many time steps, the cost per time step is that of n_φ solves of size n_r, i.e. $O(n_\varphi n_r^q)$.

For 3 DOF the complexity estimate becomes

$$C = O((n_r n_\varphi)^3 \log n_\varphi^3) + O(n_\varphi^3 n_r^{3q}).$$

Assuming that $n_r = n_\varphi = N$ we find that for $N = 50$ and $q = 1, 4/3, 2$ the cost $C = 2 \cdot 10^{11}, 9.6 \cdot 10^{11}$ and $2 \cdot 10^{15}$, respectively.

As a single modern processing unit may be able to carry out $O(10^8 - 10^9)$ arithmetic operations per second it appears plausible that an efficient parallel implementation can result in time-per-time step on the order of one to several seconds for $q = 4/3$.

Note that there are several modern solution techniques, like the Hierarchical Poincaré-Steklov operator technique by Martinsson [12] that can reach $q \approx 1$ for spectrally accurate discretizations.

NUMERICAL RESULTS

Example 1: A Single Resonance Model (SRM) in 1DOF
We now discuss the following SRM for which $d = 1$ and where $\vec{\Omega} = (\sigma_0 + \sigma_1 r \cos\varphi + \sigma_2 r \sin\varphi)(0, 0, 1)^T$. Here the reduced Bloch equations (5) can be solved exactly [13]. For example if the initial condition on $\vec{\eta}$ is chosen as $\vec{\eta}(r, \varphi, 0) = (1/\pi) \exp(-r^2)(1, 0, 0)^T$ then the polarization at time θ reads as

$$|\vec{P}(\theta)| = \exp\left\{ \frac{\pi^2 \left(\sigma_1^2 + \sigma_2^2\right)}{(a^2 + b^2)^2} \left(2\left(a^2 - b^2 - a\theta\left(a^2 + b^2\right)\right) \right.\right.$$
$$\left.\left. + 2e^{-a\theta}\left((b^2 - a^2)\cos(b\theta) + 2ab\sin(b\theta)\right)\right)\right\}. \quad (14)$$

This example was used to verify the spectral convergence of our 1DOF method outlined above (see also Example 2). In Fig. 1 we show the polarization $|\vec{P}(\theta)|$ obtained by integrating our numerical solution (see (8)). The result is very close to the exact polarization of (14), within the error we expect. In addition, the figure shows the effect of the transitional terms in (14) as well as the subsequent exponential decay of the polarization with the depolarization time τ_{dep} defined by $\tau_{dep}^{-1} = \frac{2a\pi^2(\sigma_1^2 + \sigma_2^2)}{a^2 + b^2}$.
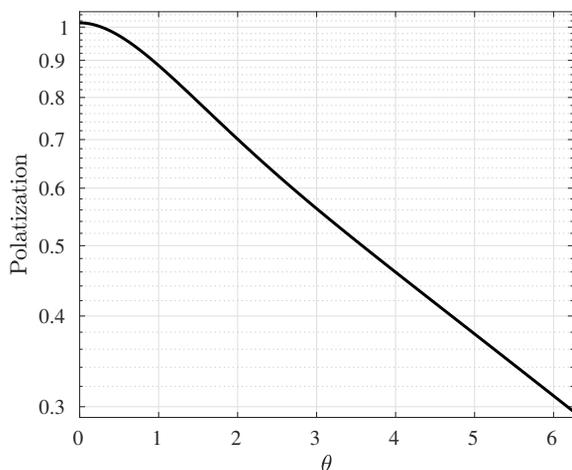

Figure 1: Polarization in SRM from numerical solution.

Example 2: Spectral convergence for 2DOF
To confirm the spectral convergence in r_1 and r_2 we evolve (5) in 2DOF with the initial data taken to be the exact solution

(obtained for constant $\vec{\Omega}$)

$$\vec{\eta}(\theta, \vec{r}, \vec{\phi}) = \exp(\mathcal{A}\theta)\,\vec{\eta}(\theta, \vec{r}, \vec{\phi}). \quad (15)$$

at $\theta = 0$. Here each component of $\vec{\eta}$ satisfies $\partial_\theta f = L_{FP} f$ which can be solved in terms of the transition probability density for a Gaussian process with easily determined mean and covariance matrix. Moreover, it has an equilibrium solution $\pi^{-2} \exp(-(r_1^2 + r_2^2))$ making it a good test case for the numerical method. To be precise, the errors displayed in Fig. 2 are the maximum deviation from the exact solution $\vec{\eta}(\theta, \vec{r}, \vec{\phi}) = \pi^{-2} \exp(-(r_1^2 + r_2^2)) \exp(\mathcal{A}\theta)(1, 1, 1)^T$, taken over all grid points and all the variables at $\theta = \pi/4$ and with $\vec{\Omega} = (0, 0, 1)^T$ and $a_1 = b_1 = a_2 = b_2 = 1$. The results clearly show the spectral accuracy of the spatial discretization as well as the second order accuracy of the temporal discretization. A similar plot was obtained for 1DOF in Example 1.
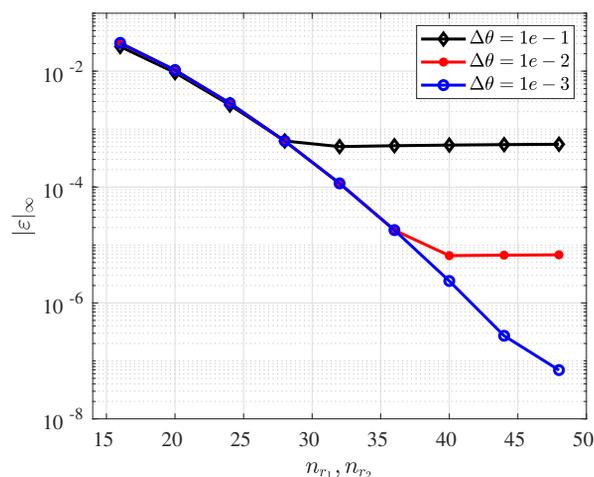

Figure 2: Convergence for 2DOF.

DISCUSSION AND NEXT STEPS

We are preparing an extended version of this brief note for an archival journal which will complete the work on the reduced Bloch equation of (5) in 2DOF. An important aspect will be a more detailed discussion of the algorithm. The codes will be made available in a repository. A goal is to make our work easily reproducible. Next we will incorporate the spin flip by considering the full Bloch equations and do a careful study of the depolarization and polarization effects for the simple lattice incorporated by the (a_l, b_l) in (6). This will include depolarization and polarization times and equilibrium. We will then study a more realistic lattice in the 2DOF case and begin the 3DOF work, where a parallel algorithm will surely be important/necessary.

ACKNOWLEDGEMENT

REFERENCES

[1] Ya.S. Derbenev, A.M. Kondratenko, "Polarization kinetics of particles in storage rings", *Sov. Phys. JETP*, vol. 37, p. 968, 1973.

[2] D.P. Barber, G. Ripken, "Radiative Polarization, Computer Algorithms and Spin Matching in Electron Storage Rings", *Handbook of Accelerator Physics and Engineering*. Eds. A.W. Chao and M. Tigner, 1st edition, 3rd printing, World Scientific, 2006. See also arXiv:physics/9907034v2

[3] Ya.S. Derbenev, A.M. Kondratenko, "Relaxation and equilibrium state of electrons in storage rings", *Sov. Phys. Dokl.*, vol. 19, p. 438, 1975,

[4] D.P. Barber, K. Heinemann, H. Mais, G. Ripken, "A Fokker-Planck treatment of stochastic particle motion", DESY-91-146, 1991.

[5] *Handbook of Accelerator Physics and Engineering*, third printing, edited by A.W. Chao, M. Tigner, 2006.

[6] M. Sands, "The physics of electron storage rings", SLAC-121, 1970. J. Jowett, "Introductory Statistical Mechanics for electron storage rings", SLAC-PUB-4033, 1986.

[7] V.N. Baier, V.M. Katkov, V.M. Strakhovenko, "Kinetics of Radiative Polarization", *Sov. Phys. JETP*, vol. 31, p. 908, 1970.

[8] F. Bloch, *Phys. Rev.*, vol. 70, p. 460, 1946.

[9] K. Heinemann, D.P. Barber, "Spin transport, spin diffusion and Bloch equations in electron storage rings", *Nucl. Instr. Meth. A*, vol. 463, pp. 62–67, 2001.Erratum-ibid.A469:294.

[10] B. Fornberg, "Classroom Note: Calculation of Weights in Finite Difference Formulas", *SIAM Review*, vol. 40(3), pp. 685–691, 1998.

[11] G.E. Karniadakis, M. Israeli, S. A Orszag, "High-order splitting methods for the incompressible Navier-Stokes equations", *J. Comput. Phys.*, vol. 97, no, 2, pp. 414–443, 1991.

[12] P.G. Martinsson, "A direct solver for variable coefficient elliptic PDEs discretized via a composite spectral collocation method", *J. Comput. Phys.*, vol. 242, pp. 460 – 479, 2013.

[13] K. Heinemann, unpublished notes.